

Technoeconomic, environmental and multi criteria decision making investigations for optimisation of off-grid hybrid renewable energy system with green hydrogen production

Dibyendu Roy, Mrinal Bhowmik^{*}, Anthony Paul Roskilly

Department of Engineering, Durham University, Durham, DH1 3LE, UK

ARTICLE INFO

Handling Editor: Giovanni Baiocchi

Keywords:

HRES
LCOE
Multi-criteria decision making
Hydrogen
Economic analysis
Biomass

ABSTRACT

The current study presents a comprehensive investigation of various energy system configurations for a remote village community in India with entirely renewable electricity. Excess electricity generated by the systems has been stored using two types of energy storage options: lithium-ion batteries and green hydrogen production through the electrolyzers. The hybrid renewable energy system (HRES) configurations have been sized by minimising the levelised cost of energy (LCOE). In order to identify the best-performing HRES configuration, economic and environmental performance indicators has been analysed using the multi-criteria decision-making method (MCDM), TOPSIS. Among the evaluated system configurations, system-1 with a photovoltaic panel (PV) size of 310.24 kW, a wind turbine (WT) size of 690 kW, a biogas generator (BG) size of 100 kW, a battery (BAT) size of 174 kWh, an electrolyser (ELEC) size of 150 kW, a hydrogen tank (HT) size of 120 kg, and a converter (CONV) size of 106.24 kW has been found to be the best-performing system since it provides the highest relative closeness (RC) value (~0.817) and also has the lowest fuel consumption rate of 2.31 kg/kWh. However, system-6 shows the highest amount of CO₂ (143.97 kg/year) among all the studied system configurations. Furthermore, a detailed technical, economic, and environmental analysis has been conducted on the optimal HRES configuration. The minimum net present cost (NPC), LCOE, and cost of hydrogen (COH) for system 1 has been estimated to be \$1,960,584, \$0.44/kWh, and \$22.3/kg, respectively.

1. Introduction

The 2021 International Energy Agency (IEA) Report (IEA, 2021) highlights that coal currently accounts for 44% of India's primary energy demand. This is a critical issue as many industries, including key sectors such as transportation and industrial production, still heavily rely on imported fossil fuels. Additionally, India's electricity consumption has nearly tripled over the past two decades (IEA, 2021), and there are projections of a significant increase in energy consumption in the coming years. The transition to clean and sustainable renewable energy technologies from traditional fossil-based energy is essential to achieve the net-zero target and simultaneously reduce greenhouse gas (GHG) emissions (D'Adamo et al., 2020). This energy transition not only facilitates private investment with the goal of generating job opportunities (Adamo et al., 2022) but also contributes significantly to economic and social progress (Falcone, 2023), fostering economic development with a focus on sustainability (Lopolito et al., 2022). Furthermore, the

COVID-19 pandemic has expedited the shift in both power generation and primary energy mix, steering away from carbon-intensive sources towards modern renewables, aligning with a more sustainable energy future (K. Li et al., 2022). In this regard, the scope of green finance could play a major role in scaling up sustainable projects (Falcone, 2024). It provides necessary capital for renewable energy projects, thus leveraging financial markets for sustainable development (Patrizio, 2022).

Given India's commitment to achieving net zero emissions by 2070, there is a need for significant changes in the country's energy consumption patterns. To address this, India has launched its National Green Hydrogen Mission, which aims to develop the necessary infrastructure to produce at least 5 million metric tons of green hydrogen annually by 2030 (MNRE, 2023). One potential solution in this context is the use of renewable energy-based green hydrogen. Hybridization of various renewable energy sources for electricity production at the demand site, along with the production of green hydrogen using any

^{*} Corresponding author.

E-mail addresses: dibyendu.roy@durham.ac.uk (D. Roy), mrinal.bhowmik@durham.ac.uk (M. Bhowmik).

<https://doi.org/10.1016/j.jclepro.2024.141033>

Received 29 September 2023; Received in revised form 27 December 2023; Accepted 29 January 2024

Available online 7 February 2024

0959-6526/© 2024 The Authors. Published by Elsevier Ltd. This is an open access article under the CC BY license (<http://creativecommons.org/licenses/by/4.0/>).

available excess electricity, could be an alternative option. The application of hybrid renewable energy systems (HRES) is specifically appropriate for rural and remote regions in India. Although these areas have gained access to electrical networks, they still experience frequent power outages. Adopting an off-grid HRES approach could present a more practical solution, leading to decreased operational costs, lower emissions, improved energy efficiency, and enhanced system dependability (Mansouri et al., 2022).

Numerous studies have explored the techno-economic viability of HRES in various locations. For instance, Pan et al. (2023) investigated a HRES that integrated photovoltaic-wind turbine and battery technologies into the power grid. They employed an improved grey wolf optimisation algorithm and reported a 41.9% reduction in the system cost compared to the grid-based system without the HRES. Roy (2023) investigated an off-grid hybrid renewable energy system modelled for a remote village in the Sundarbans, using machine learning techniques and reported the lowest LCOE of 0.31 \$/kWh with a combination of a diesel generator (DG), wind turbine (WT), photovoltaic (PV) panel, battery (BAT), and a converter (CONV)-based system. Xu et al. (2023) investigated PV-WT-BAT and biogas generator (BG) integrated HRES in some Chinese urban communities and reported lowest LCOE of 0.27 \$/kWh. Das et al. (2022) investigated the use of HRES with different energy storage devices and reported the corresponding LCOE and renewable fraction (RF) for the optimal solution as \$0.197/kWh, and

89.17%, respectively. Afif et al. (2023) investigated PV,WT,BG, BAT, CONV and flywheel integrated HRES configurations with for Jordan's Al-Karak governorate. They reported lowest LCOE and RF of 0.024 \$/kWh and 71.8%, respectively, can be achieved. Kumar et al. (2023) conducted a study on a system based on PV, micro hydro, BAT, and biomass gasifier for a rural community in India. They employed techno-economic and socio-economic analyses and reported LCOE in the range of INR 3.93 to 4.23 per kWh. Izadi et al. (2022) modelled a HRES configuration based on PV-WT, fuel cell, electrolyser (ELEC), and hydrogen storage for a building, and further investigated it using a neural network genetic algorithm. Their results suggest that the genetic algorithm with a population size of 50 gave an optimum configuration of 291 PV panels and one WT, which produced CO₂ emissions of 53.48 tonnes per year, and the cost rate of the system is 1.42 €/hour.

Table 1 and previous discussion indicate that previous studies have primarily focused on using batteries as a means to utilise excess electricity in HRES-based systems. However, only a few studies have explored the potential for hydrogen production from this excess electricity. Therefore, the objective of this research is to examine the viability of HRES configurations that include different configurations of PV, WT, BG, lithium-ion BAT, CONV, ELEC, and hydrogen tanks (HT) for the Netsi village community in Rajasthan, India. Systems were modelled using MATLAB software, and the sizing of the HRES configurations was accomplished by minimisation of levelised cost of energy. To identify

Table 1
Summary of recent studies related to HRES.

System configuration	Study location	Excess energy storage option	Study type				Key results	Ref.
			Technical	Economic	Environmental	MCDM		
PV/WT/BAT/BG/CONV	Tehran, Iran	Lithium-ion battery	✓	✓	✓	×	The system's LCOE for the optimum configuration was reported as \$0.28 per kWh.	Hossein Jahangir et al. (2022)
PV/WT/BAT/CONV/Grid	Jakhau, India	Battery	✓	✓	✓	×	LCOE ranged from \$0.040 to \$0.097 per kWh, also enabling a 5.4–6.6 million kg CO ₂ equivalent reduction annually compared to standalone grid power.	Memon et al. (2021)
PV/WT/DG/CONV/Grid	Konya, Turkey	Lithium-ion battery	✓	✓	✓	×	The minimum LCOE reported for on-grid and off-grid studies is \$0.18/kWh and \$0.321/kWh, respectively.	Gügül (2023)
PV/BAT/FC/ELEC/CONV/HT	Bhopal, India	lead-acid battery, and hydrogen	✓	✓	×	×	The LCOE of the system was reported as \$0.20 per kWh.	Singh et al. (2017)
PV/WT/DG/BAT/Grid	Valencia, Spain	Battery	✓	✓	✓	×	The results showed full demand coverage in all scenarios, with a maximum power loss of 4.5% and battery SOC ranging from 35% to 100%.	Bastida-Molina et al. (2021)
PV/WT/DG/BAT/CONV/Grid	Kenya	Battery	✓	✓	✓	✓	The lowest NPC was reported as 2.6 M\$, and the lowest LCOE was 0.28 \$/kWh.	Elkadeem et al. (2021)
PV/BG/BAT/CONV	West Bengal, India	Lithium-ion battery	✓	✓	✓	×	LCOE was reported in the range of \$0.101 to \$0.105 per kWh.	Das and Mandal (2022)
PV/WT/BAT/MGT/CONV/Electric Boiler/Gas Boiler	Broome, Australia	Lithium-ion battery	✓	✓	✓	×	The optimal configuration excels with a \$0.17/kWh cost of energy, a 25,220 kg/yr carbon footprint, and a 92.85% renewable fraction.	Hassan et al. (2022)
PV/WT/DG/BAT/RO/CONV	Kutubdia Island, Bangladesh	Lead-acid battery	✓	✓	✓	×	The optimum system was able to provide an LCOE of \$0.234/kWh, 1.64 jobs, and 24,038 kWh/yr of excess energy.	(P. Das et al., 2022)
DG/WT/PV/BAT/CONV	Kerman province, Iran	Lithium-ion battery	✓	✓	×	×	The minimum LCOE was reported to be \$0.12/kWh with an 80% renewable fraction	Amin et al. (2024)
PV/DG/BAT/CONV	Luxor, Egypt	Lead-acid battery	✓	✓	×	×	The LCOE was reported to be \$0.26 per kWh	Elfatah et al. (2023)
PV/WT/CONV/BAT/FC	Gwadar Port, Pakistan, and Salalah Port, Oman	Lead-acid battery and Lithium-ion battery	✓	✓	✓	×	The configuration of the lithium-ion battery system provides an economical LCOE of \$0.295/kWh.	Iqbal et al. (2023)

PV: Photovoltaic panel, WT: Wind turbine, BAT: Battery, CONV: Converter, FC: Fuel cell, HT: Hydrogen Tank, DG: Diesel generator, BG: Biogas generator, RO: Reverse osmosis, ELEC: Electrolyser, NPC: Net present cost, LCOE: Levelised cost of energy, SOC: State of charge.

the best performing HRES configuration, economic and environmental performance indicators are analysed by applying the multi-criteria decision-making method TOPSIS. Furthermore, a detailed technical, economic, and environmental analysis has been performed on the optimal HRES configuration.

The major contributions of the study are outlined below.

- Proposal of seven distinct HRES configurations, incorporating combinations of photovoltaic panels (PV), wind turbines (WT), biogas generators (BG), lithium-ion batteries (BAT), converters (CONV), electrolyzers (ELEC), and hydrogen tanks (HT).
- Identification of the best-performing HRES configuration through the analysis of economic and environmental performance indicators using the multi-criteria decision-making method.
- The use of the TOPSIS method for analysing the economic and environmental performance of various HRES configurations is employed. This method provides a more holistic and balanced evaluation of the systems, considering multiple criteria that are critical for the real-world implementation of these systems.
- The detailed economic analysis, including the calculation of the net present cost (NPC), levelised cost of energy (LCOE), and cost of hydrogen (COH), offers new insights into the financial viability of HRES in rural settings. This aspect is crucial for the scalability and adoption of such systems in similar contexts.
- The current study extends the environmental assessment of HRES by quantifying CO₂ emissions for each system configuration. This comprehensive environmental impact assessment, particularly in the context of hydrogen production from surplus electricity, is a significant addition to the existing literature.

2. Material and methods

2.1. Location of the study

The selected location of the study is Netsi village, located in the Jaisalmer district of Rajasthan, India, as depicted in Fig. 1. As per the Census of 2011, the total population of the area is 967 individuals (VillageInfo, 2024). Table 2 outlines the community's electrical load for the study location.

Solar data was obtained from NASA databases, and Fig. 2 illustrates the monthly solar radiation and clearness index observed at Netsi

village. The monthly solar radiation varies between 3.44 kWh/m²/day to 6.59 kWh/m²/day, with an estimated average of 5.13 kWh/m²/day throughout the year. The solar radiation data considered for the analysis represents an average over a 22-year period, spanning from July 1983 to June 2005. June exhibits the highest levels of solar radiation, while December displays the lowest radiation intensity. In addition, the clearness index in August is observed to be at its lowest, measuring 0.53, whereas February records the highest value of 0.6.

Wind velocity information for the study area was acquired from NASA databases and displayed in Fig. 3. The minimum wind speed was recorded in November at 3.59 m/s, while the maximum wind speed of 7.30 m/s was observed in June across different months in Netsi village. The wind speed data utilised in the analysis reflects an average over a 30-year period, extending from January 1984 to December 2013. The wind turbine has a cut-in speed of 2.75 m/s and a cut-out wind speed of 20 m/s for the analysis (Duman and Güler, 2018). In addition, Fig. 4 illustrates the average daily biomass available on the left axis and the mean temperature at the location on the right axis. Mustard crop residue and Juliflora serve as significant biomass feeds readily accessible in Rajasthan, making them well-suited for the energy system. Additionally, the system can effectively operate with other local biomass feeds, including various agricultural wastes such as cotton stalks, paddy straw, and maize stalks (RREC, 2021).

2.2. System topology

In order to ensure that the energy system is optimised for the specific needs of the village, careful consideration must be given to the selection and arrangement of these components. By selecting the right combination of components and ensuring efficient utilisation, it is possible to create a sustainable and cost-effective energy system for the village. The HRES configurations are designed with different combinations of components, including photovoltaic panels (PV), wind turbines (WT), biogas generators (BG), lithium-ion batteries (BAT), converters (CONV), electrolyzers (ELEC), and hydrogen tanks (HT). The primary objective of these systems is to meet the electricity demand of the village, with any excess energy generated being stored in the BATs or used to produce hydrogen through the electrolyzers. Fig. 5 depicts the proposed configuration of the HRES.

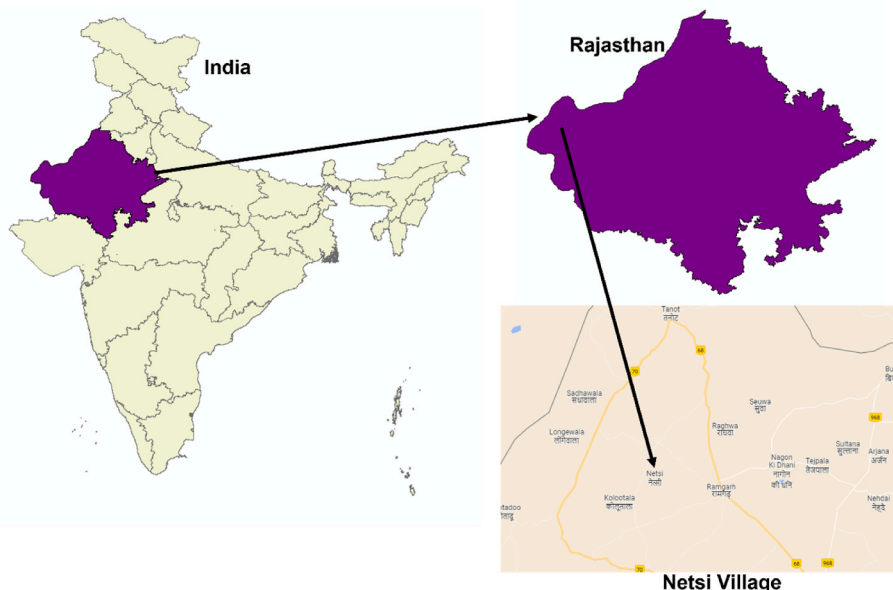


Fig. 1. Location of the study.

Table 2
Electric demand at the study location.

Load category	Room/Building configuration	Appliances	Quantity	Watt	Usage (h)	Load (W.h/d)	Total category (kWh/d)
Primary school	4 classrooms	CFL bulb	10	25	8	2000	5.973
		Fan	5	70	8	2800	
	1 Office	Computer	1	100	8	800	
		Water pump	1	746	0.5	373	
		CFL bulb	8	25	7	1400	
Household	2 Rooms	Fan	2	70	7	980	931.5
		External Lighting	1	100	6	600	
	1 Kitchen	TV	1	100	6	600	
		Water Pump	1	746	1	746	
		CFL bulb	8	25	7	1400	
Total Number of houses (250)							
Primary Health center	3 Wards	CFL	30	25	8	6000	23.2
		Fan	15	70	8	8400	
	2 Offices	Computer	2	100	8	1600	
		Refrigerator	2	150	24	7200	
		CFL	20	25	8	4000	
Business center	10 Small Shops	Fan	14	70	8	7840	58.84
		Computer	12	100	8	9600	
	1 Post Office	Refrigerator	10	150	24	36000	
		TV	2	100	7	1400	
		CFL	35	25	8	7000	
Streetlights						7	
Total demand							1026.5

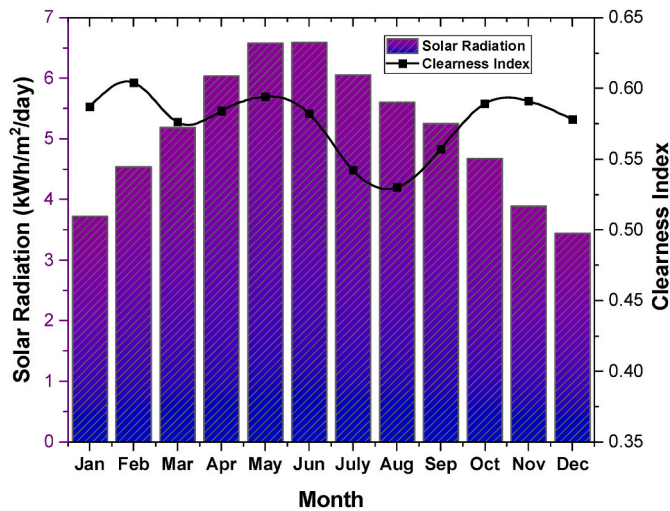


Fig. 2. Monthly solar radiation and clearness index at the study location.

2.3. System components

2.3.1. Photovoltaic array

The estimation of the power generated by the photovoltaic array can be computed by Eq. (1) (Mousavi et al., 2021).

$$\dot{W}_{PV} = Z_{PV} \times FD_{PV} \times \left(\frac{\bar{I}_T}{\bar{I}_{T,STC}} \right) \times (1 + \beta_t (T_C - T_{C,STC})) \quad (1)$$

The symbols employed in the aforementioned expression have the following connotations: Z_{PV} corresponds to the rated capacity of the photovoltaic (PV) array, whereas FD_{PV} is the PV derating factor. The term \bar{I}_T represents the solar radiation incident on the PV array during the present time step, while $\bar{I}_{T,STC}$ denotes the incident radiation at standard test conditions. The parameter β_t indicates the temperature coefficient of power, and T_C represents the temperature of the PV cell at the present time step and, $T_{C,STC}$ denotes the temperature of the cell under standard test conditions. Equation (2) can be used to estimate the cell temperature (Mousavi et al., 2021)

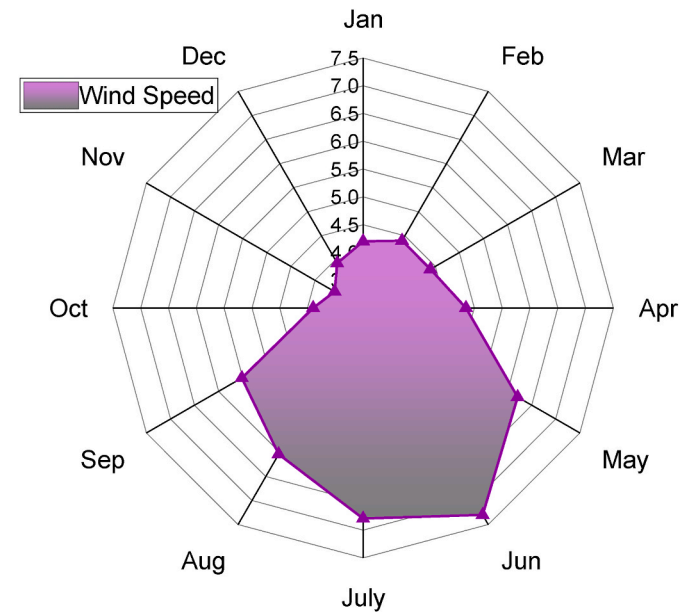


Fig. 3. Average monthly wind speed at the location of the study.

$$T_c = \frac{T_a + (T_{C,NOCT} - T_{a,NOCT}) \left(\frac{\bar{I}_T}{\bar{I}_{T,STC}} \right) \left(1 - \frac{\eta_{MP,STC} (1 - \beta_t \times T_{C,STC})}{\alpha} \right)}{1 + (T_{C,NOCT} - T_{a,NOCT}) \left(\frac{\bar{I}_T}{\bar{I}_{T,STC}} \right) \left(\frac{\beta_t \times \eta_{MP,STC}}{\alpha} \right)} \quad (2)$$

The parameters $T_{C,NOCT}$ and $T_{a,NOCT}$ are used to represent the nominal operating cell temperature and atmospheric temperature, respectively. Additionally, the expression $\eta_{MP,STC}$ denotes the maximum power efficiency achieved under standard test conditions, while β_t corresponds to the temperature coefficient of power.

Equation (3) is used to estimate the energy generated by the PV arrays (Mousavi et al., 2021)

$$E_{PV} = N_{PV} \times \dot{W}_{PV} (t) \times \Delta t \quad (3)$$

where, Δt denotes the time-period and is 1 h.

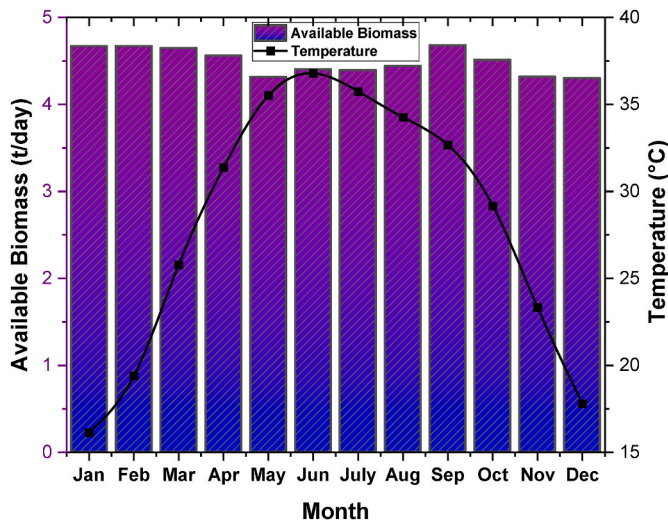


Fig. 4. Monthly biomass availability and temperature at the location of the study.

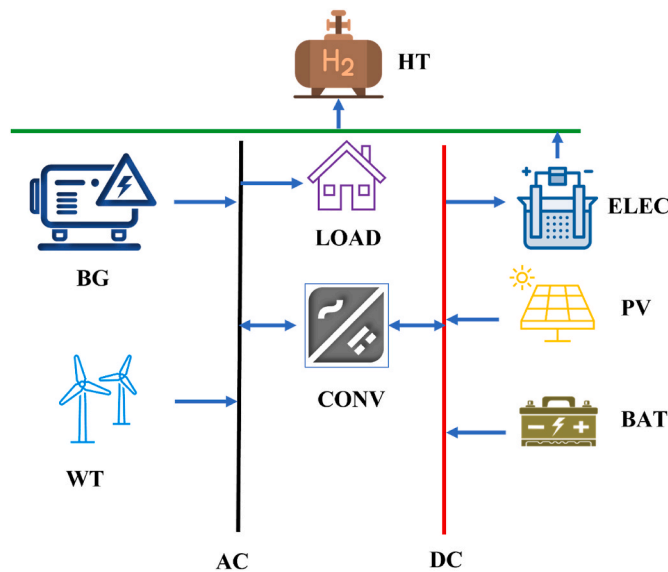


Fig. 5. Schematic of the proposed hybrid renewable energy system.

2.3.2. Wind turbine

The power output of wind turbines can be estimated by Eq. (4) (Mousavi et al., 2021).

$$\bar{W}_{WT} = \begin{cases} 0; & V \leq V_{cut,in} \\ a \times V^3 - b \times \dot{W}_{rated}; & V_{cut,in} \leq V \leq V_{rated} \\ \dot{W}_{rated}; & V_{rated} \leq V \leq V_{cut,off} \\ 0; & V > V_{cut,off} \end{cases} \quad (4)$$

where Eqs. (5) and (6) can be utilised to determine the values of both ‘a’ and ‘b’. (Mousavi et al., 2021)

$$a = \frac{\dot{W}_{rated}}{V_{rated}^3 - V_{cut,in}^3} \quad (5)$$

$$b = \frac{V_{cut,in}^3}{V_{rated}^3 - V_{cut,in}^3} \quad (6)$$

where \dot{W}_{rated} , $V_{cut,in}$, V_{rated} and $V_{cut,off}$ are the rated power, cut-in wind speed, rated wind velocity, and cut-off wind velocity, respectively.

2.3.3. Battery bank

The reliability of an energy system can be improved by integrating battery storage facilities, according to Alsagri et al. (2021). These facilities are commonly used to supply electricity during times of peak demand or when renewable energy sources are unavailable. In this study, lithium-ion batteries have been employed as they efficiently store excess energy during the charging process.

2.3.4. Biomass generator

The electrical efficiency of the biomass generator can be expressed by Eq. (7) (Kumar and Koteswara Rao, 2022).

$$\eta_{BG} = \frac{3.6 \times P_{BG}}{\dot{m}_{fuel} \times LHV_{fuel}} \quad (7)$$

where, \dot{m}_{fuel} is the mass flowrate of fuel, P_{BG} is the power output of the generator, and LHV_{fuel} denotes lower heating value of the fuel.

2.3.5. Electrolyser

In the present study, a polymer electrolyte membrane (PEM) type electrolyser has been considered. PEM electrolyser produces green hydrogen by consuming excess electricity generated by the system. Furthermore, as part of the National Green Hydrogen mission, India aims to develop a green hydrogen production capacity of at least 5 million metric tonnes per annum by 2030 (MNRE, 2023). The PEM electrolyser operates at lower temperatures and is already a well-established technology. Local manufacturers in India also make PEM electrolysers, making it a suitable choice for this study (GreenH, 2023). The cathode and anode reactions are provided below (Rad et al., 2020).



2.4. Economic analysis

In order to evaluate the economic performance, the present study utilised the net present cost (NPC) and levelised cost of energy (LCOE) as crucial performance parameters. The total NPC was calculated using the mathematical expression presented in Eq. (10) (Elmorshedy et al., 2021).

$$NPC = CAP + OM + RC + SL \quad (10)$$

Eq. (10) is used for determining the total NPC incorporates four different cost elements, which are denoted as CAP, OM, RC, and SL. These cost components include capital costs, operating costs, replacement costs, and salvage costs, respectively.

The expression for the system’s capital cost (CAP) component is presented in Eq. (11) (Elmorshedy et al., 2021).

$$CAP = \sum_{k=1}^{N_{comp}} N_k CAP_k \quad (11)$$

The calculation for the CAP of the system involves the multiplication of the number of components, represented by N_k , with the corresponding capital cost of the kth component, denoted as CAP_k .

In order to determine the operating and maintenance cost (OM) of the system, Eq. (12) can be utilised (Elmorshedy et al., 2021).

$$OM = \sum_{k \in comp} \sum_{y=1}^{T_{proj}} \frac{1}{\left[1 + \left(\frac{d_n - f_r}{1 + f_r}\right)^y\right]} N_k \times OM_k \quad (12)$$

Eq. (12) involves the use of several variables, including, OM_k , which represents the operation and management cost of the kth component. Other variables in the formula include, d_n , which denotes the real discount rate (expressed as a percentage), f_r , which stands for the inflation

rate (also as a percentage), and T_{Proj} , which indicates the project lifetime in years.

The replacement cost (RPC) component of the system can be calculated using Eq. (13) (Elmorshedy et al., 2021):

$$RPC = \sum \frac{1}{\left[1 + \left(\frac{d_n - f_c}{1 + f_r}\right)\right]^{T_k}} N_k \times RPC_k \quad (13)$$

The parameters T_k and C_k , respectively, represent the component lifetime in years and the total replacement cost of the component.

The computation of the total salvage cost (SL) of the system is carried out using Eq. (14) (Elmorshedy et al., 2021):

$$SL = \sum_{k \in comp} \frac{1}{\left[1 + \left(\frac{d_n - f_c}{1 + f_r}\right)\right]^{T_k}} \times \frac{T_{k,rem}}{T_k} \times N_k \times SL_k \quad (14)$$

where the remaining lifespan of the kth component is denoted as $T_{k,rem}$ and the salvage cost of the same component is represented as SL_k .

The determination of the total annual cost (C_{annual}) is presented in Eq. (15).

$$C_{annual} = NPC \times CRF \quad (15)$$

The parameter CRF denotes the capital recovery factor, which is calculated by the equation given below:

$$CRF = \frac{\left(\frac{d_n - f_c}{1 + f_r}\right) \times \left[1 + \left(\frac{d_n - f_c}{1 + f_r}\right)\right]^p}{\left[1 + \left(\frac{d_n - f_c}{1 + f_r}\right)\right]^{T_{Proj}} - 1} \quad (16)$$

The levelised cost of energy (LCOE) is the minimum cost necessary to sell electricity at a breakeven cost over the lifetime of the HRES. It is mathematically expressed as Eq. (17) (Elmorshedy et al., 2021):

$$LCOE = \frac{C_{annual}}{E_{GEN}} \quad (17)$$

The parameters C_{annual} and E_{GEN} denote the total annual cost (expressed in \$/year) and total annual electricity production (expressed in kWh/year), respectively.

3. Results and discussion

3.1. Technical performance comparison between different configurations

Technoeconomic input parameters considered for the analysis are provided in Table 3. The sizing of different system configurations is provided in Table 4. The largest PV size is observed in System 4, while System 3 comes in second place, followed by System 2, System 1, and finally, System 6. System 5 has the largest WT size, followed by System 7, System 1, System 6, and System 2 in that order. System 4 has the maximum Lithium-ion battery size, followed by System 2, System 3, System 1, and System 5, respectively. System 5 has the highest CONV size. System 6 and System 7 have the highest BG size (150 kW), while System 2, System 3, and System 5 have the maximum electrolyser size.

The highest amount of excess electricity production is contributed by System 5 (72.6%), followed by System 4 (62.2%), System 3 (58.5%), System 7 (54.2%), System 1 (53.4%), System 2 (50.1%), and System 6 (44%), respectively. System 5 has the maximum capacity shortage, around 349 kWh/year. Among the systems, System 6 consumes the highest amount of biogas at 2.37kg/kWh, while System 1 has the lowest consumption rate at 2.31kg/kWh. Since System 2 and System 4 do not integrate biogas generator, their fuel consumption is zero. Notably, these findings illuminate not only the substantial variations in excess electricity production and capacity shortages among the systems, but also the diverse patterns in biogas consumption, underscoring the

Table 3
Techno-economic specifications of components.

Component	Parameters	Data	Ref
PV	Rated capacity	1 kW	(Akhtari et al., 2020; Khan et al., 2022; J. Li et al., 2022a)
	Derating factor	80%	
	Rated voltage	54.7 V	
	Temperature coefficient	-0.5/°C	
	Efficiency	13%	
	Operating Temperature	47 °C	
	Rated current	5.98A	
	Efficiency	13%	
	Capital cost	\$900/kW	
	Replacement cost	\$850/kW	
	OM cost	\$10/kW	
	Lifetime	20 years	
	Power rating	10 kW	
	Capital cost	\$9500/kW	
WT	Replacement cost	\$9000/kW	(J. Li et al., 2022a)
	OM cost	\$30/year	
	Lifetime	30 years	
	Voltage rating	6 V	
Battery	Nominal capacity	1 kWh	(J. Li et al., 2022a)
	Roundtrip efficiency	90%	
	Maximum charge current	167 A	
	Maximum discharge current	500 A	
	Capital cost	\$500 per unit	
	Replacement cost	\$500 per unit	
Converter	OM cost	\$5 per year	(J. Li et al., 2022a)
	Lifetime	15 years	
	Power rating	1 kW	
	Inverter efficiency	95%	
	Rectifier efficiency	95%	
	Capital cost	\$300/kW	
BG	Replacement cost	\$300/kW	(J. Li et al., 2022a)
	OM cost	3\$/year	
	Lifetime	15 years	
	Power rating	1 kW	
	Minimum load ratio	25%	
	Fuel cost	100\$/t	
	Biogas LHV	5.5 MJ/kg	
	Biogas density	0.720 kg/m ³	
	Capital cost	\$550/unit	
	Replacement cost	\$550/unit	
Electrolyser	OM cost	0.05 \$/hour	(J. Li et al., 2022a)
	Lifetime	15000 h	
	Efficiency	85%	
Hydrogen tank	Capital cost	\$1500/unit	(J. Li et al., 2022a)
	Replacement cost	\$1000/unit	
	OM cost	\$20/year	
	Lifetime	15 years	
	Capacity	1 kg	
	Capital cost	\$600/unit	
Hydrogen tank	Replacement cost	\$450/unit	(J. Li et al., 2022a)
	OM cost	\$10/year	
Hydrogen tank	Lifetime	20 years	(J. Li et al., 2022a)

Table 4
Technical details of the different system configurations.

	PV (kW)	WT (kW)	BG (kW)	BAT (kWh)	ELEC (kW)	HT (kg)	CONV (kW)
System 1	310.24	690.00	100.00	174.00	150.00	120.00	106.24
System 2	454.98	530.00		883.00	200.00	140.00	141.38
System 3	1267.68		50.00	725.00	200.00	150.00	104.03
System 4	1396.78			910.00	150.00	150.00	145.03
System 5		1700.00	100.00	167.00	200.00	150.00	235.23
System 6	134.44	550.00	150.00		150.00	40.00	43.95
System 7		880.00	150.00		150.00	150.00	148.86

nuanced dynamics within the energy production landscape.

3.2. Application of TOPSIS multi-criteria decision making method to prioritise HRES

The multi-criteria decision-making method, TOPSIS, has been applied using MATLAB software to obtain the best-performing HRES configuration among the seven HRES configurations. The decision parameters chosen for analysis are NPC, LCOE, capital cost (CC), replacement cost (RPC), cost of hydrogen (COH), and CO₂ emission. The decision variables for the TOPSIS analysis has been provided in Table 5.

The normalised decision matrix (M_{ij}) has been estimated by vector normalisation (Kumar et al., 2017).

$$M_{ij} = \left[\frac{x_{ij}}{\sqrt{\sum_{i=1}^n x_{ij}^2}} \right] \quad (\text{for } j = 1, 2, \dots, m) \tag{18}$$

Equal weights method has been considered and the weighted normalised matrix is determined by Eq.(19) (Kumar and Channi, 2022)

$$Z_{ij} = w_j \times M_{ij} \tag{19}$$

where w_j is the weights and it is estimated as follows (Kumar et al., 2017)

$$w_j (\text{for } j = 1, 2, \dots, m) = \frac{1}{m} \tag{20}$$

as there are 6 attributes are considered, the above equation can be written as follows

$$w_j (\text{for } j = 1, 2, \dots, m) = \frac{1}{6} \tag{21}$$

The ideal best solutions are determined by the following equations (Kumar et al., 2017)

Table 5
Decision variables for multi-criteria decision-making.

	NPC (\$)	LCOE (\$/kWh)	CC (\$)	RPC (\$)	COH (\$/kg)	CO ₂ Emission (kg/year)
System 1	1960584	0.44	1405588	17936.12	22.3	28.27
System 2	2226542	0.50	1780897	16378.95	25.3	0.00
System 3	2620550	0.59	1952119	22983.87	29.7	3.03
System 4	2704118	0.61	2070613	23452.91	30.7	0.00
System 5	2808025	0.63	2214070	20305.70	31.9	34.00
System 6	2891083	0.65	988179	49906.22	33.3	143.97
System 7	3025417	0.68	1278158	46669.08	34.7	132.69

$$Z_j^+ = [best (Z_{ij})]_{i=1}^n \tag{22}$$

$$Z^+ = [Z_1^+, Z_2^+, \dots, Z_j^+, \dots, Z_m^+] \tag{23}$$

for $j = 1, 2, 3 \dots, m$, where each j is linked to a beneficial attribute, Z^+ represents the best possible value of that attribute.

The ideal worst solutions are determined by the following equations (Kumar et al., 2017)

$$Z_j^- = [worst (Z_{ij})]_{i=1}^n \tag{24}$$

$$Z^- = [Z_1^-, Z_2^-, \dots, Z_j^-, \dots, Z_m^+] \tag{25}$$

for $j = 1, 2, 3 \dots, m$ where each j is linked to a non-beneficial attribute, Z^- represents the worst possible value of that attribute.

The Euclidean distance can be used to determine the degree of separation between each alternative and the ideal solution, which can be expressed as follows (Kumar et al., 2017):

$$S_i^+ = \sqrt{\sum_{j=1}^m (Z_{ij} - Z^+)^2} \tag{26}$$

$$S_i^- = \sqrt{\sum_{j=1}^m (Z_{ij} - Z^-)^2} \tag{27}$$

The proximity of a specific alternative to an ideal solution can be expressed as follows

$$RC_i = \frac{S_i^-}{S_i^+ + S_i^-} \tag{28}$$

The values of separation measures and relative closeness of all the systems are provided in Table 6. Based on RC values System 1 has the maximum value of 0.817, thus, it is chosen as the best system configuration.

3.3. Performance analysis of the optimal HRES configuration

In this subsection, the performance of system 1 has been discussed in detail. Fig. 6 (a) shows the power output of the photovoltaic (PV) system, wind turbine (WT), and biomass gasifier (BG), as well as the electricity load served. On the other hand, Fig. 6 (b) displays the hydrogen load and electrolyser hydrogen output.

Table 6
Ranking of different case studies.

	S_i^+	S_i^-	RC	Rank
System 1	0.029	0.128	0.817	1
System 2	0.032	0.143	0.815	2
System 3	0.048	0.131	0.731	3
System 4	0.054	0.132	0.711	4
System 5	0.066	0.110	0.625	5
System 6	0.143	0.047	0.249	6
System 7	0.134	0.038	0.249	7

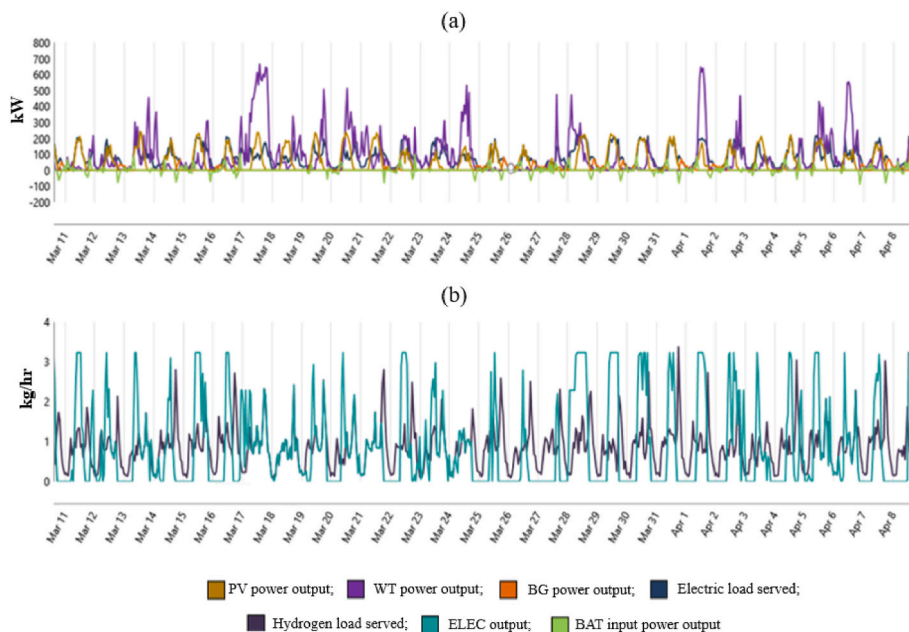


Fig. 6. (a) Power sources (b) Hydrogen load and Electrolyser output.

Fig. 7 illustrates the net present cost breakdown of the capital cost, replacement cost, operation and management cost, fuel cost, and salvage cost for case study 1. It is noteworthy that the wind turbine (WT) incurs the highest capital cost (47%), followed by PV (20%), ELEC (16%), BAT (6%), HT (5%), BG (4%), and CONV (2%). The wind turbine's larger size, reaching a peak capacity of 690 kW, significantly contributes to its elevated capital cost. Regarding replacement cost, PV accounts for the largest share (28%), followed by BAT (24%), ELEC (22%), BG (15%), HT (6%), and CONV (5%). As for operation and management cost, BG incurs the highest expense (41.1%), followed by PV (17.3%), ELEC (16.7%), WT (11.3%), HT (6.7%), BAT (4.9%), and CONV (1.8%). The total fuel cost is projected to be \$186,252.67, primarily attributed to biomass consumption in the BG unit. In terms of salvage cost, PV has the highest cost (40%), followed by WT (21%), BAT (14%), ELEC (10%), HT (8%), BG (5%), and CONV (2%). Furthermore, exploring the implications of these cost breakdowns, it becomes evident that the distribution underscores critical considerations for decision-makers, emphasising the diverse financial commitments associated with each component throughout the lifecycle of the energy system in Case Study 1.

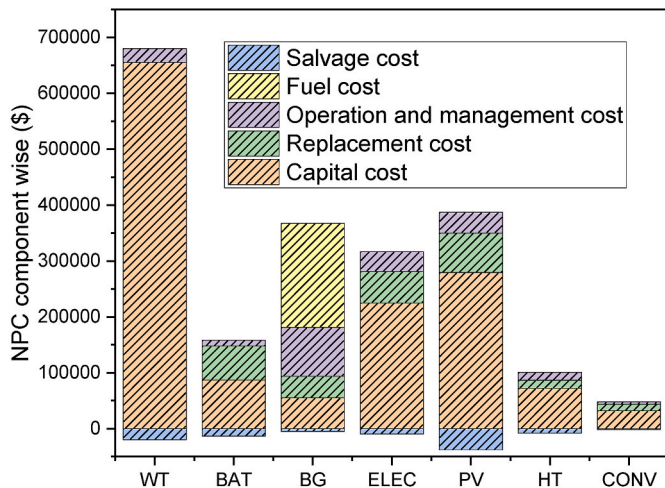


Fig. 7. Net present cost component wise Capital cost, replacement cost, operation and management cost, fuel cost and salvage cost.

Fig. 8 illustrates the emissions of various species, including CO₂, CO, and NO_x. It demonstrates that, among these emission components, CO₂ emissions (27.3 kg/year) are the highest in comparison to CO and NO_x emissions. Specifically, CO emissions stand at 2 g/kg of biomass consumed, while NO_x emissions are recorded at 1.25 g/kg of biomass consumed.

3.4. Comparisons of present work with previous studies

In this subsection, the results of the proposed system are compared with previous relevant studies, and the findings are presented in Table 7. The proposed configuration demonstrated a comparable LCOE to other configurations. In terms of CO₂ emissions, the proposed configuration even outperformed some of the previous studies.

4. Conclusion

In the current study, an in-depth analysis was conducted for various

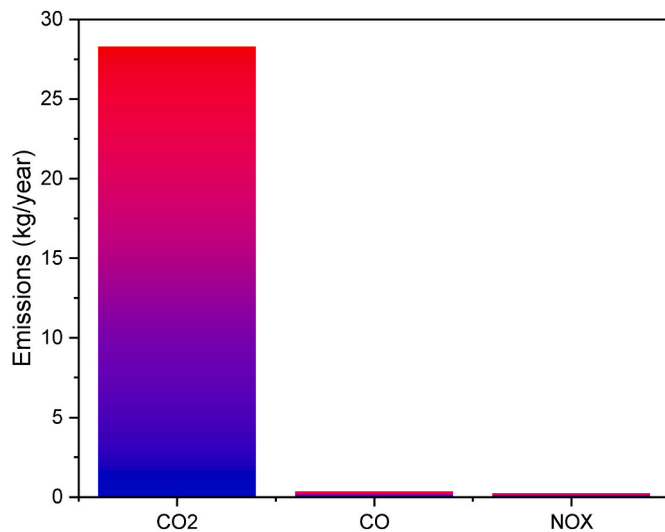


Fig. 8. Emissions from case study 1.

Table 7
Performance comparison with previous relevant studies.

System configuration	Study location	LCOE (\$/kWh)	CO ₂ emission (kg/year)	Reference
PV, WT, ELEC, Lithium-ion BAT, HT, CONV integrated system.	North America	0.60-0.78	–	Abdolmaleki and Berardi (2023)
PV, WT, Diesel Generator, BAT, CONV, ELEC, HT integrated system.	Diyala, Muqdadiah district, Iraq	0.244	1856	J. Li et al. (2022b)
PV, WT, BG, BAT, CONV, ELEC, HT integrated system.	Healthcare centers during the Corona pandemic	0.348	–	Hossein Jahangir et al. (2023)
PV, WT, ELEC, Lithium-ion BAT, HT, CONV integrated system.	Geelong, Victoria, Australia	0.4347	–	Okonkwo (2023)
PV, hydrogen fuel cell (HFC), ELEC, lead-acid BAT, HT and CONV integrated system.	Energy Centre, Maulana Azad National Institute of Technology, Bhopal, India	0.20	–	Singh et al. (2017)
PV, BG, Lithium-ion BAT, WT, ELEC-HT, CONV integrated system.	Netsi village, Rajasthan, India	0.440	28.27	Present study

energy system configurations for providing electricity from renewable sources and to produce green hydrogen for a remote village community in India. Excess electricity generated by the systems was stored using lithium-ion batteries and used to generate green hydrogen. The HRES configurations were sized by minimising the levelised cost of energy. In order to identify the best-performing HRES configuration, economic and environmental performance indicators were analysed using the multi-criteria decision-making method, TOPSIS. Additionally, a detailed technical, economic, and environmental analysis was performed for the optimal HRES configuration. The main findings of the study are as follows.

- System 1 with PV: 310.24 kW, WT: 690 kW, BG: 100 kW, BAT: 174 kWh, ELEC: 150 kW, HT: 120 kg, and CONV: 106.24 kW has the lowest fuel consumption rate at 2.31 kg/kWh among all the evaluated system configurations.
- The multi-criteria decision-making method also suggests that System 1 is the optimal configuration since its RC value (0.817) is the highest among the other studied systems.
- The minimum net present cost (NPC), levelised cost of energy (LCOE), and cost of hydrogen (COH) for system 1 are estimated to be \$1,960,584, \$0.44/kWh, and \$22.3/kg, respectively.
- System 6 emits the highest amount of CO₂ (143.97 kg/year) among all the studied system configurations.

The developed design methodology not only offers a comprehensive guideline for designing hybrid renewable energy systems (HRES), but also underscores the imperative of sustainability by providing a framework to evaluate various configurations that contribute to the advancement of sustainable energy solutions. This model is a valuable

reference tool for evaluating various system configurations within an integrated framework. In essence, the developed model and methodology can estimate the optimal configuration and thoroughly assess the system characteristics of HRES installations. These contributions will aid researchers, engineers, and policymakers in making informed decisions and advancing the field of sustainable energy. Furthermore, HRES has the potential to attract investment through the green finance route. For future research endeavours, this study could be expanded by incorporating a thorough life cycle assessment (LCA) to investigate detailed environmental assessments. Additionally, investigations into the resilience and reliability aspects also need to be conducted, considering factors such as extreme weather events, equipment failures, and challenges related to maintenance.

CRediT authorship contribution statement

Dibyendu Roy: Conceptualization, Data curation, Formal analysis, Investigation, Methodology, Resources, Software, Validation, Visualization, Writing – original draft, Writing – review & editing. **Mrinal Bhowmik:** Conceptualization, Formal analysis, Investigation, Methodology, Software, Validation, Visualization, Writing – review & editing. **Anthony Paul Roskilly:** Formal analysis, Funding acquisition, Project administration, Supervision, Writing – review & editing, Resources.

Declaration of competing interest

The authors declare that they have no known competing financial interests or personal relationships that could have appeared to influence the work reported in this paper.

Data availability

Data will be made available on request.

Acknowledgments

This research was delivered with financial support from the UK Research Council (UKRI) for a project entitled “Zero-Carbon Emission Integrated Cooling, Heating and Power (ICHPP) Networks” (EP/T022949/1).

Appendix A. Supplementary data

Supplementary data to this article can be found online at <https://doi.org/10.1016/j.jclepro.2024.141033>.

References

- Abdolmaleki, L., Berardi, U., 2023. International Journal of Hydrogen Energy Hybrid solar energy systems with hydrogen and electrical energy storage for a single house and a midrise apartment in North America. *Int. J. Hydrogen Energy*. <https://doi.org/10.1016/j.ijhydene.2023.11.222>.
- Adamo, I.D., Falcone, P.M., Imbert, E., Morone, P., 2022. Exploring Regional Transitions to the Bioeconomy Using a Socio - Economic Indicator : the Case of Italy, *Economia Politica*. Springer International Publishing. <https://doi.org/10.1007/s40888-020-00206-4>.
- Akhtari, M.R., Shayegh, I., Karimi, N., 2020. Techno-economic assessment and optimization of a hybrid renewable earth - air heat exchanger coupled with electric boiler, hydrogen, wind and PV configurations. *Renew. Energy* 148, 839–851. <https://doi.org/10.1016/j.renene.2019.10.169>.
- Al Afif, R., Ayed, Y., Maaitah, O.N., 2023. Feasibility and optimal sizing analysis of hybrid renewable energy systems: a case study of Al-Karak, Jordan. *Renew. Energy* 204, 229–249. <https://doi.org/10.1016/j.renene.2022.12.109>.
- Alsagri, A.S., Alrobaian, A.A., Nejlou, M., 2021. Techno-economic evaluation of an off-grid health clinic considering the current and future energy challenges: a rural case study. *Renew. Energy* 169, 34–52. <https://doi.org/10.1016/j.renene.2021.01.017>.
- Amin, M., Rad, V., Kasaeian, A., 2024. Evaluation of stand-alone hybrid renewable energy system with excess electricity minimizer predictive dispatch strategy Lower Heating Value of Fuel State of Charge. *Energy Convers. Manag.* 299, 117898 <https://doi.org/10.1016/j.enconman.2023.117898>.

- Bastida-Molina, P., Hurtado-Pérez, E., Moros Gómez, M.C., Vargas-Salgado, C., 2021. Multicriteria power generation planning and experimental verification of hybrid renewable energy systems for fast electric vehicle charging stations. *Renew. Energy* 179, 737–755. <https://doi.org/10.1016/j.renene.2021.07.002>.
- D'Adamo, I., Falcone, P.M., Gastaldi, M., Morone, P., 2020. The economic viability of photovoltaic systems in public buildings: Evidence from Italy. *Energy* 207, 118316. <https://doi.org/10.1016/j.energy.2020.118316>.
- Das, M., Mandal, R., 2022. The effect of photovoltaic energy penetration on a Photovoltaic-Biomass-Lithium-ion off-grid system and system optimization for the agro-climatic zones of West Bengal. *Sustain. Energy Technol. Assessments* 53, 102593. <https://doi.org/10.1016/j.seta.2022.102593>.
- Das, P., Das, B.K., Rahman, M., Hassan, R., 2022. Evaluating the prospect of utilizing excess energy and creating employments from a hybrid energy system meeting electricity and freshwater demands using multi-objective evolutionary algorithms. *Energy* 238. <https://doi.org/10.1016/j.energy.2021.121860>.
- Das, S., Ray, A., De, S., 2022. Comparative analysis of storage modules under different dispatch strategies for an optimum decentralized hybrid energy solution: a case study of a remote Indian village. *Clean Technol. Environ. Policy* 24, 2495–2515. <https://doi.org/10.1007/s10098-022-02330-0>.
- Duman, A.C., Güler, Ö., 2018. Techno-economic analysis of off-grid PV/wind/fuel cell hybrid system combinations with a comparison of regularly and seasonally occupied households. *Sustain. Cities Soc.* 42, 107–126. <https://doi.org/10.1016/j.scs.2018.06.029>.
- Elfatah, A.A., Hashim, F.A., Mostafa, R.R., El-Sattar, H.A., Kamel, S., 2023. Energy management of hybrid PV/diesel/battery systems: a modified flow direction algorithm for optimal sizing design — a case study in Luxor, Egypt. *Renew. Energy* 218, 119333. <https://doi.org/10.1016/j.renene.2023.119333>.
- Elkadeem, M.R., Younes, A., Sharshir, S.W., Campana, P.E., Wang, S., 2021. Sustainable siting and design optimization of hybrid renewable energy system: a geospatial multi-criteria analysis. *Appl. Energy* 295, 117071. <https://doi.org/10.1016/j.apenergy.2021.117071>.
- Elmorshedy, M.F., Elkadeem, M.R., Kotb, K.M., Taha, I.B.M., Mazzeo, D., 2021. Optimal design and energy management of an isolated fully renewable energy system integrating batteries and supercapacitors. *Energy Convers. Manag.* 245, 114584. <https://doi.org/10.1016/j.enconman.2021.114584>.
- Falcone, M., 2024. *Sustainable Finance and the Global Health Crisis*. Taylor & Francis.
- Falcone, P.M., 2023. *Sustainable Energy Policies in Developing Countries : A Review of Challenges and Opportunities*.
- GreenH, 2023. GreenH Electrolysis announces its first 1 GW PEM electrolyser manufacturing plant in India [WWW Document]. URL <https://greenh.in/GreenH-Electrolysis-Announces-its-First-1-GW-PEM-Electrolyser-Manufacturing-Plant-in-India/index.html>.
- Gügül, G.N., 2023. Optimum hybrid renewable energy system design for on and off grid buildings: hotel, education and animal hospital building case. *Sol. Energy* 253, 414–427. <https://doi.org/10.1016/j.solener.2022.12.044>.
- Hassan, R., Das, B.K., Al-Abdeli, Y.M., 2022. Investigation of a hybrid renewable-based grid-independent electricity-heat nexus: impacts of recovery and thermally storing waste heat and electricity. *Energy Convers. Manag.* 252, 115073. <https://doi.org/10.1016/j.enconman.2021.115073>.
- Hossein Jahangir, M., Bazdar, E., Kargarzadeh, A., 2022. Techno-economic and environmental assessment of low carbon hybrid renewable electric systems for urban energy planning: tehran-Iran. *City Environ. Interact.* 16, 100085. <https://doi.org/10.1016/j.cacint.2022.100085>.
- Hossein Jahangir, M., Eslamnezhad, S., Kargarzadeh, A., 2023. Designing reliable energy hubs for healthcare centers during the Corona pandemic using hybrid optimization methods and deep analysis. *Clean. Mater.* 7, 100178. <https://doi.org/10.1016/j.clema.2023.100178>.
- IEA, 2021. *India Energy Outlook, World Energy Outlook Special Report*.
- Iqbal, R., Liu, Y., Zeng, Y., Zhang, Q., Zeeshan, M., 2023. Comparative study based on techno-economics analysis of different shipboard microgrid systems comprising PV/wind/fuel cell/battery/diesel generator with two battery technologies: a step toward green maritime transportation. *Renew. Energy*, 119670. <https://doi.org/10.1016/j.renene.2023.119670>.
- Izadi, A., Shahafve, M., Ahmadi, P., 2022. Neural network genetic algorithm optimization of a transient hybrid renewable energy system with solar/wind and hydrogen storage system for zero energy buildings at various climate conditions. *Energy Convers. Manag.* 260, 115593. <https://doi.org/10.1016/j.enconman.2022.115593>.
- Khan, F.A., Pal, N., Saeed, S.H., Yadav, A., 2022. Modelling and techno-economic analysis of standalone SPV/Wind hybrid renewable energy system with lead-acid battery technology for rural applications. *J. Energy Storage* 55, 105742. <https://doi.org/10.1016/j.est.2022.105742>.
- Kumar, N., Namrata, K., Samadhiya, A., 2023. Techno socio-economic analysis and stratified assessment of hybrid renewable energy systems for electrification of rural community. *Sustain. Energy Technol. Assessments* 55, 102950. <https://doi.org/10.1016/j.seta.2022.102950>.
- Kumar, R., Bilga, P.S., Singh, S., 2017. Multi objective optimization using different methods of assigning weights to energy consumption responses, surface roughness and material removal rate during rough turning operation. *J. Clean. Prod.* 164, 45–57. <https://doi.org/10.1016/j.jclepro.2017.06.077>.
- Kumar, R., Channi, H.K., 2022. A PV-Biomass off-grid hybrid renewable energy system (HRES) for rural electrification: design, optimization and techno-economic-environmental analysis. *J. Clean. Prod.* 349, 131347. <https://doi.org/10.1016/j.jclepro.2022.131347>.
- Kumar, S., Koteswara Rao, S., 2022. Optimum capacity of hybrid renewable energy system suitable for fulfilling yearly load demand for a community building located at Vaddeswaram, Andhra Pradesh. *Energy Build.* 277, 112570. <https://doi.org/10.1016/j.enbuild.2022.112570>.
- Li, J., Liu, P., Li, Z., 2022a. Optimal design and techno-economic analysis of a hybrid renewable energy system for off-grid power supply and hydrogen production: a case study of West China. *Chem. Eng. Res. Des.* 177, 604–614. <https://doi.org/10.1016/j.cherd.2021.11.014>.
- Li, J., Liu, P., Li, Z., 2022b. Optimal design of a hybrid renewable energy system with grid connection and comparison of techno-economic performances with an off-grid system: a case study of West China. *Comput. Chem. Eng.* 159, 107657. <https://doi.org/10.1016/j.compchemeng.2022.107657>.
- Li, K., Qi, S., Shi, X., 2022. The COVID-19 pandemic and energy transitions: evidence from low-carbon power generation in China. *J. Clean. Prod.* 368, 132994. <https://doi.org/10.1016/j.jclepro.2022.132994>.
- Lopolito, A., Falcone, P.M., Sica, E., 2022. The role of proximity in sustainability transitions: a technological niche evolution analysis. *Res. Policy* 51, 104464. <https://doi.org/10.1016/j.respol.2021.104464>.
- Mansouri, S.A., Ahmarinejad, A., Nematbakhsh, E., Javadi, M.S., Esmael Nezhad, A., Catalão, J.P.S., 2022. A sustainable framework for multi-microgrids energy management in automated distribution network by considering smart homes and high penetration of renewable energy resources. *Energy* 245. <https://doi.org/10.1016/j.energy.2022.123228>.
- Memon, S.A., Upadhyay, D.S., Patel, R.N., 2021. Optimal configuration of solar and wind-based hybrid renewable energy system with and without energy storage including environmental and social criteria: a case study. *J. Energy Storage* 44, 103446. <https://doi.org/10.1016/j.est.2021.103446>.
- MNRE, 2023. National green hydrogen mission [WWW Document]. URL <https://mnre.gov.in/national-green-hydrogen-mission/#:~:text=The National Green Hydrogen Mission,efficiently transport and distribute hydrogen>.
- Mousavi, S.A., Zarchi, R.A., Astaraei, F.R., Ghasempour, R., Khaninezhad, F.M., 2021. Decision-making between renewable energy configurations and grid extension to simultaneously supply electrical power and fresh water in remote villages for five different climate zones. *J. Clean. Prod.* 279, 123617. <https://doi.org/10.1016/j.jclepro.2020.123617>.
- Okonkwo, P.C., 2023. A case study on hydrogen refueling station techno-economic viability. *Int. J. Hydrogen Energy.* <https://doi.org/10.1016/j.ijhydene.2023.11.086>.
- Pan, T., Wang, Z., Tao, J., Zhang, H., 2023. Operating strategy for grid-connected solar-wind-battery hybrid systems using improved grey wolf optimization. *Electr. Power Syst. Res.* 220, 109346. <https://doi.org/10.1016/j.epr.2023.109346>.
- Patrizio, G., 2022. Scaling up of green finance in a post-COVID-19 era: a sustainability transition perspective and policy insights. *IGI Global.* <https://doi.org/10.4018/978-1-7998-8501-6.ch004>.
- Rad, M.A.V., Ghasempour, R., Rahdan, P., Mousavi, S., Arastounia, M., 2020. Techno-economic analysis of a hybrid power system based on the cost-effective hydrogen production method for rural electrification, a case study in Iran. *Energy* 190, 116421. <https://doi.org/10.1016/j.energy.2019.116421>.
- Roy, D., 2023. Modelling an off-grid hybrid renewable energy system to deliver electricity to a remote Indian island. *Energy Convers. Manag.* 281, 116839. <https://doi.org/10.1016/j.enconman.2023.116839>.
- RREC, 2021. *Biomass Assessment Study for Power Generation in Rajasthan for Rajasthan. Renewable Energy Corporation*.
- Singh, A., Baredar, P., Gupta, B., 2017. Techno-economic feasibility analysis of hydrogen fuel cell and solar photovoltaic hybrid renewable energy system for academic research building. *Energy Convers. Manag.* 145, 398–414. <https://doi.org/10.1016/j.enconman.2017.05.014>.
- VillageInfo, 2024. *Netsi, INDIAN VILLAGE DIRECTORY* [WWW Document]. VillageInfo. URL <https://villageinfo.in/rajasthan/jaisalmer/jaisalmer/netsi.html>.
- Xu, X., Zhang, Z., Yuan, J., Shao, J., 2023. Design and multi-objective comprehensive evaluation analysis of PV-WT-BG-Battery hybrid renewable energy systems in urban communities. *Energy Convers. Manag.* X 18, 100357. <https://doi.org/10.1016/j.ecmx.2023.100357>.